

# Directional statistics for WIMP direct detection

Ben Morgan,<sup>1</sup> Anne M. Green,<sup>2</sup> and Neil J. C. Spooner<sup>1</sup>

<sup>1</sup>*Department of Physics and Astronomy, University of Sheffield,  
Hicks Building, Hounsfield Road, Sheffield, S3 7RH, United Kingdom*

<sup>2</sup>*Department of Physics and Astronomy, University of Sheffield, Hicks Building,  
Hounsfield Road, Sheffield, S3 7RH, United Kingdom (present address)  
and Astronomy Centre, University of Sussex, Brighton BN1 9QH, United Kingdom  
and Physics Department, Stockholm University, Stockholm, S106 91, Sweden*

(Dated: May 23, 2019)

The direction dependence of the event rate in WIMP direct detection experiments provides a powerful tool for distinguishing WIMP events from potential backgrounds. We use a variety of (non-parametric) statistical tests to examine the number of events required to distinguish a WIMP signal from an isotropic background when the uncertainty in the reconstruction of the nuclear recoil direction is included in the calculation of the expected signal. We consider a range of models for the Milky Way halo, and also study rotational symmetry tests aimed at detecting non-sphericity/isotropy of the Milky Way halo. Finally we examine ways of detecting streams of WIMPs, such as that expected from the Sagittarius dwarf tidal stream. We find that if the senses of the recoils are known then of order ten events will be sufficient to distinguish a WIMP signal from an isotropic background for all of the halo models considered, with the uncertainties in reconstructing the recoil direction only mildly increasing the required number of events. If the senses of the recoils are not known the number of events required is an order of magnitude larger, with a large variation between halo models, and the recoil resolution is now an important factor. The rotational symmetry tests require of order a thousand events to distinguish between spherical and significantly triaxial halos, however a deviation of the peak recoil direction from the direction of the solar motion due to the Sagittarius tidal stream could be detected with of order a hundred events, regardless of whether the sense of the recoils is known.

PACS numbers: 95.35.+d

astro-ph/0408047

## I. INTRODUCTION

Weakly Interacting Massive Particle (WIMP) direct detection experiments aim to directly detect non-baryonic dark matter via the elastic scattering of WIMPs on detector nuclei, and are presently reaching the sensitivity required to detect neutralinos (the lightest supersymmetric particle and an excellent WIMP candidate). Since the expected event rates are very small ( $\mathcal{O}(10^{-5} - 1)$  counts  $\text{kg}^{-1}\text{day}^{-1}$ ) distinguishing a putative Weakly Interacting Massive Particle (WIMP) signal from backgrounds due to, for instance, neutrons from cosmic-ray induced muons or natural radioactivity, is crucial. The Earth's motion about the Sun provides two potential WIMP smoking guns: i) an annual modulation [1] and ii) a strong direction dependence [2] of the event rate. In principle the dependence of the differential event rate on the atomic mass of the detector (see e.g. Refs. [3, 4]) is a third possibility, however this would require good control of systematics for detectors composed of different materials.

The DAMA (DARK MATter) collaboration have, using  $\sim 100$  kg of NaI crystals and an exposure of  $\sim 1.1 \times 10^5$  kg day, observed an annual modulation in their event rate [5], which they interpret as a WIMP signal. Taken at face value the allowed region of WIMP mass and cross-section parameter space is incompatible with the exclusion limits from other experiments (such as the Cryogenic Dark Matter Search, Edelweiss and Zeplin

I) [6], however the form of the WIMP annual modulation signal, in particular its phase, depends sensitively on the local WIMP velocity distribution [7, 8, 9, 10]<sup>1</sup>. It is, however, difficult to exclude the possibility that the annual modulation could be due to some previously unidentified background.

The direction dependence of the WIMP scattering rate has several advantages over the annual modulation. Firstly, the amplitude of the annual modulation is typically of order a few per-cent [1, 4] while the event rate in the forward direction is roughly an order of magnitude larger than that in the backward direction [2, 4]. Secondly it is difficult for the directional signal to be mimicked by backgrounds; in most cases (a point source in the lab is a possible exception) a background which is anisotropic in the laboratory frame will be isotropic in the Galactic rest frame as the, time dependent, conversion between the lab and Galactic co-ordinate frames will wash out any lab specific features. Furthermore the mean direction, in the lab, of WIMP induced recoils will vary over a sidereal day due to the rotation of the Earth [13]. Designing a detector capable of measuring the directions of sub-100keV nuclear recoils is however a considerable

<sup>1</sup> Other theoretical possibilities which could perhaps resolve this conflict include spin-dependent interactions [11] and inelastic scattering [12].

challenge. Prototype directional detectors based on roton anisotropy in liquid He [14], phonon anisotropy in BaF crystals [15] and the anisotropic scintillation properties of stilbene [16] have been tested, however low pressure gas time projection chambers (TPCs), such as DRIFT (**D**irectional **R**ecoil **I**dentification **F**rom **T**racks) [17, 18], seem to offer the best prospects for a workable detector. In discriminating a WIMP signal from isotropic backgrounds it is therefore crucial to take into account the accuracy with which recoil directions can be measured by such a detector. Furthermore, the direction dependence of the recoil rate depends on the local WIMP velocity distribution [19]. Whilst this opens up the exciting possibility of experimentally probing the local dark matter distribution if WIMPs are detected (i.e. doing WIMP astronomy), it is also crucial that uncertainties in this distribution are accounted for when designing tests for discriminating a WIMP signal from isotropic backgrounds.

Earlier studies have found that as few as 30 events would be required to distinguish a WIMP induced signal from isotropic backgrounds [19, 20] and that with of order hundreds of events it may be possible to distinguish between different models for the Galactic halo [19]. In this paper we improve on these works by including the uncertainty in the reconstruction of the nuclear recoil direction and applying non-parametric tests to unbinned data. In Sec. II we describe our calculation of the nuclear recoil spectrum, including the modelling of the Milky Way halo (Sec. II A) and the reconstruction of the recoil direction (Sec. II B). In Sec. III we then study an array of statistical tests aimed at probing the isotropy (Sec. III B and Sec III A), rotational symmetry (Sec. III C) and mean direction (Sec. III D) of a putative WIMP directional signal.

## II. CALCULATING THE NUCLEAR RECOIL SPECTRUM

### A. Modelling the Milky Way halo

The simplest possible model of the Milky Way (MW) halo is an isotropic sphere with density distribution  $\rho \propto r^{-2}$ , in which case the velocity distribution at all position within the halo is maxwellian:

$$f_0(\vec{v}) = \frac{1}{(2\pi/3)^{3/2}\sigma_0^3} \exp\left(-\frac{3|\vec{v}|^2}{2\sigma_0^2}\right), \quad (1)$$

where  $\sigma_0$ , the velocity dispersion, is related to the asymptotic circular velocity (which we take throughout to be  $v_c = 220\text{kms}^{-1}$ ) by  $\sigma_0 = \sqrt{3/2}v_c$ .

Observations and numerical simulations indicate that galaxy halos are in fact triaxial and anisotropic and contain substructure. Numerical simulations produce both prolate ( $c/b > b/a$ ) and oblate ( $c/b < b/a$ ) halos (where  $(a, b, c)$  are the lengths of the long, intermediate and short principal axes of the density distribution respectively) [21, 22]. To date only cluster sized halos have

been simulated in large numbers. Ref. [22] found that the shape parameters of such large halos lie in the ranges  $c/a \sim 0.4 - 0.6$  and  $b/a \sim 0.7 - 0.8$ . However the axial ratios vary with radius within a given halo, depending at least partly on the merger history of the halo. Ref. [23] studied two high resolution simulations of MW size halos, one halo had  $c/a \sim b/a \sim 0.4$ , the other  $c/a \sim 0.5$  and  $b/a \sim 0.8$ . These simulations contain only collisionless matter, and the addition of baryons leads to halos that are less triaxial, especially in the central regions [24]. These ranges of axial ratios are in rough agreement with observational measurements of the shape of dark matter halos (for reviews see e.g. Ref. [25]).

The two MW-like halos in Ref. [23] have velocity anisotropy at the solar radius ( $r = R_0 \approx 8\text{kpc}$ )  $\beta(R_0) \sim 0.3 \pm 0.1$  where  $\beta$  is defined as:

$$\beta(r) = 1 - \frac{\langle v_\theta^2 \rangle + \langle v_\phi^2 \rangle}{2\langle v_r^2 \rangle}, \quad (2)$$

where  $\langle v_\theta^2 \rangle$ ,  $\langle v_\phi^2 \rangle$  and  $\langle v_r^2 \rangle$  are the mean square velocity components in Galactic co-ordinates.

### 1. Triaxial and anisotropic models

We consider two anisotropic and/or triaxial halo models: the logarithmic ellipsoidal model [26, 27] and the Osipkov-Merritt model [28, 29]. We summarise these models briefly below. For further details see either the original papers [27, 28, 29] or Refs. [30] and [31].

The logarithmic ellipsoidal model [26, 27] is the simplest triaxial, scale free generalisation of the isothermal sphere, its shape and velocity anisotropy being independent of radius. This model was studied in detail, in the context of WIMP direct detection, by Evans, Carollo and de Zeeuw [27] and has since been used widely in calculations of the expected WIMP signals [8, 10, 31]. In this model, it is assumed that the principle axes of the velocity distribution are aligned with conical co-ordinates, and in any of the planes of the halo conical co-ordinates coincide with local cylindrical polar co-ordinates and the local WIMP distribution can be approximated by a multivariate Gaussian:

$$f_0(\vec{v}) = \frac{1}{(2\pi)^{3/2}\sigma_R\sigma_\phi\sigma_z} \exp\left(-\frac{v_R^2}{2\sigma_R^2} - \frac{v_\phi^2}{2\sigma_\phi^2} - \frac{v_z^2}{2\sigma_z^2}\right), \quad (3)$$

where  $(\sigma_R, \sigma_\phi, \sigma_z)$  are the radial, azimuthal and polar velocity dispersions respectively. These dispersions are given in terms of parameters  $p$  and  $q$  that are related to the halo axis ratios and  $\gamma$  which is related to the isotropy parameter  $\beta$  [27, 31].

Osipkov-Merritt models [28, 29] provide self-consistent radially anisotropic velocity distribution functions for halos with spherically symmetric density profiles, with velocity anisotropy  $\beta(r) = r^2/(r^2 + r_a^2)$  where  $r_a$  is the anisotropy radius. We follow Ref. [30] and assume that

the MW has an NFW profile [32] with scale radius  $20\text{kpc}$ <sup>2</sup> and fix  $r_a = 20$  and  $12\text{kpc}$  as in Ref. [31], corresponding to  $\beta(R_0) = 0.14$  and  $0.31$ , and calculate the local velocity distribution using the fitting functions in Ref. [33].

The parameters of the fiducial halo models which we consider are chosen to span the range of halo properties discussed above and are summarised in Table I. Some of the triaxial models (numbers 6-9) are rather extreme (with  $\sigma_z \ll \sigma_r, \sigma_\phi$ ), however they serve as a best/worse case scenario allow us to assess whether the deviation of the recoil spectrum from that produced by the standard halo is detectable/problematic.

## 2. Sagittarius dwarf tidal stream

The extent to which the local WIMP distribution is smooth is an open question [23, 34, 35, 36], however it is certainly possible that a stream of high velocity particles from a late accreted sub-halo could be passing through the solar neighbourhood [34, 35]. Indeed one of the tidal tails of the Sagittarius dwarf satellite galaxy (Sgr), which is in the process of being tidally disrupted, is thought to pass close to the solar system [37, 38]. As dark matter would also be stripped from the Sgr dwarf, a tidal stream of WIMPs may pass through the solar system [39, 40]. This stream therefore provides an observationally well motivated example to use to assess the effect of a tidal stream on the directional signal.

Freese et al. [40] argue that a group of halo stars in the solar neighbourhood, moving coherently with mean velocity in Galactic coordinates  $\vec{v}_{\text{str}} = (-65.0, 135.0, -249.0)\text{km s}^{-1}$  are associated with the Sgr tidal stream. We follow Ref. [39, 40] and model the velocity distribution of WIMPs in the stream in the solar neighbourhood with a maxwellian distribution with bulk velocity  $\vec{v}_{\text{str}}$ , and velocity dispersion  $\sigma_{\text{str}}$ :

$$f_0(\vec{v}) = \frac{1}{(2\pi/3)^{3/2}\sigma_{\text{str}}^3} \exp\left(-\frac{3|\vec{v} - \vec{v}_{\text{str}}|^2}{2\sigma_{\text{str}}^2}\right). \quad (4)$$

We take  $\sigma_{\text{str}} = 30\text{km s}^{-1}$ , and  $\rho_0 = 0.07\text{GeV cm}^{-3}(\approx 0.25\rho_0)$ , (towards the lower and upper ends of the range of values suggested in Ref. [39, 40] respectively and therefore providing a best case scenario for detectability), and for simplicity use the standard maxwellian velocity distribution [eq. (1)] for the smooth background component.

No.	Type	p	q	$\beta$	axis	$\rho_{\text{str}}/\rho_0$	$\sigma_{\text{str}}$ (km s <sup>-1</sup> )
1	SHM	-	-	-	-	-	-
2	LGE	0.9	0.8	0.1	I	-	-
3	LGE	0.9	0.8	0.4	I	-	-
4	LGE	0.9	0.8	0.1	L	-	-
5	LGE	0.9	0.8	0.4	L	-	-
6	LGE	0.72	0.7	0.1	I	-	-
7	LGE	0.72	0.7	0.4	I	-	-
8	LGE	0.72	0.7	0.1	L	-	-
9	LGE	0.72	0.7	0.4	L	-	-
10	OM	-	-	0.31	-	-	-
11	OM	-	-	0.14	-	-	-
12	SHM.+Sgr	-	-	-	-	0.25	30

TABLE I: Summary of the parameters of the fiducial halo models. ‘SHM’ denotes the standard halo model, ‘LGE’ the logarithmic ellipsoidal model with the Sun located on either the long (L) or intermediate (I) axis, ‘OM’ the Osipkov-Merritt model and ‘SHM+ Sgr’ the standard halo model plus the Sagittarius tidal stream contributing  $\rho_{\text{str}}/\rho_0$  of the local WIMP density, with a maxwellian velocity distribution with dispersion  $\sigma_{\text{str}}$ . In each case we take  $v_c = 220\text{km s}^{-1}$  and  $\beta$  is the anisotropy parameter, defined as in eq. (2).

## B. Modelling the detector response

TPC based detectors are designed to measure the directions of nuclear recoils by drifting the ionisation produced by recoils in the gas volume to a suitable charge readout plane. The difference in ionisation track lengths between electrons, alpha particles and nuclear recoils at low gas pressure allows efficient rejection of these backgrounds [17]. To reduce charge diffusion along the track (which would restrict the spatial resolution and hence direction measurement and background discrimination) to thermal levels the detector can be filled with an electronegative gas to give negative ion drift. The DRIFT collaboration have adopted CS<sub>2</sub> as a suitable electronegative gas; for further details see Ref. [17, 18].

Multiple scattering of the recoiling nucleus together with the small, but finite, diffusion of drifted ionisation limits the accuracy with which the direction of the primary recoil can be reconstructed. In order to assess the likely accuracy of the track reconstruction we consider a TPC detector filled with 0.05 bar CS<sub>2</sub> with a 200  $\mu\text{m}$  pitch micropixel readout plane, a 10cm drift length over which a uniform electric field of  $1\text{kV cm}^{-1}$  is applied, and a 20keV primary recoil energy threshold. This gas pressure, mixture and electric field are chosen to match the design of the DRIFT-I detector [18]. The micropixel readout is based on those described in Ref. [41], and the drift length is such that the rms diffusion over the full drift length is approximately equal to the pixel pitch [42].

<sup>2</sup> The exact choice of profile has little influence on the local velocity distribution [30]; at the solar radius the slope is close to  $-2$  whatever profile is used.

We use the SRIM2003 package [43]<sup>3</sup> to generate sulfur ionisation recoil tracks<sup>4</sup> and simulate the drift and diffusion of the ionisation to the readout plane under the electric field and the subsequent generation of charge avalanches. The nuclear recoil directions are then reconstructed from the resulting pixel outputs via a moment analysis and we include this uncertainty, which is typically of order  $10^\circ$ , in our Monte Carlo simulations. With SRIM2003 generated recoils, we find near uniform distributions of ionisation along the tracks and therefore cannot determine the absolute signs of the reconstructed recoil vectors (i.e.  $+\vec{x}$  or  $-\vec{x}$ ). However, we note that experimental measurements are really required to determine whether this absolute sign can be measured or not. We consider both possibilities below.

We assume that the time-dependent conversion of recoil directions measured in the laboratory frame to the galactic frame introduces no further errors in the measured recoil directions due to, for instance, inaccuracy in the measured time of the event.

We calculate the directional recoil rate above the 20 keV detector energy threshold via Monte Carlo simulation so as to allow the inclusion of the detector resolution effects discussed above. We work in Galactic  $(R, \phi, z)$  co-ordinates, where  $R$  is directed towards the Galactic center,  $\phi$  is in the direction of motion of the Local Standard of Rest (LSR) and  $z$  points towards the north Galactic pole. These co-ordinates are related to Galactic longitude  $l$  and latitude  $b$  by  $(R, \phi, z) = (\cos l \cos b, \sin l \cos b, \sin b)$ .

Firstly the WIMP velocity distribution has to be transformed to the rest frame of the detector [ $f_0(\vec{v}_\chi) \rightarrow f_\oplus(\vec{u}_\chi)$ ] via the Galilean transformation:  $\vec{v}_\chi = \vec{u}_\chi + \vec{v}_\oplus(t)$ . The velocity of the Earth,  $\vec{v}_\oplus(t)$ , is the sum of the velocity of the LSR,  $\vec{\Theta}_{LSR}$ , the peculiar velocity of the Sun,  $\vec{v}_{\odot p}$ , and the Earth's orbital velocity about the Sun,  $\vec{v}_{orb}(t)$ . We take  $\vec{\Theta}_{LSR} = 220 \text{ km s}^{-1}$  (see e.g. [44]),  $\vec{v}_{\odot p} = (10.0, 7.3, 5.2) \text{ km s}^{-1}$  [45], and use the results of the calculation of the Earth's orbital velocity detailed in Appendix A. The resulting WIMP velocity distribution in the detector rest frame is used to generate random incident WIMP velocities from the WIMP flux  $u_\chi f_\oplus(\vec{u}_\chi)$ , which then undergo isotropic scattering in the center of mass frame. We weight each recoil by a factor equal to the detector form factor (which is taken to have the Helm form appropriate for spin independent WIMP-sulfur scattering [4]) in order to take into account the variation of the scattering cross section with the momen-

tum transfer to the nucleus. Finally we include the effects of multiple scattering on the reconstructed recoil direction.

The resultant, time averaged, WIMP and recoil distributions are shown as Hammer-Aitoff projections of the flux/rate in Galactic coordinates in Figs. 1-3 for models 1 (standard halo model), 3 (logarithmic ellipsoidal model with  $p = 0.9, q = 0.8$  and  $\beta = 0.4$ ) and 12 (standard halo model with a 25% contribution to the local WIMP density from the Sagittarius dwarf tidal stream). For illustrative purposes we take  $\rho_0 = 0.3 \text{ GeV cm}^{-3}$ ,  $m_\chi = 100 \text{ GeV}$  and for the recoil flux take the WIMP-proton elastic scattering cross-section to be  $\sigma_{\chi p} = 10^{-6} \text{ pb}$ . Note the different scale for model 12. We see that the WIMP flux produced by the triaxial halo model is significantly flattened with respect to the Galactic plane, however due to the finite detector resolution the difference between the recoil rates predicted by models 1 and 3 is far smaller than the difference in the WIMP fluxes. For model 12, with the Sagittarius tidal stream the peak direction of the WIMP flux and recoil rate both differ significantly from the direction of motion of the Sun, suggesting that WIMPs from the Sagittarius dwarf could be easily detectable in a directional detector if the stream density is sufficiently large.

### III. STATISTICAL TESTS

A WIMP search strategy with a directional detector can essentially be divided into three regimes. Firstly, there is the simple search phase which aims to detect an anomalous recoil signal above that expected from backgrounds. For zero background, to claim an anomalous signal inconsistent with zero at 95% confidence requires 4-5 events. Secondly, following the discovery of an anomalous recoil signal, there would be the confirmation stage. At this point the experiment would collect more data and aim to confirm the recoil signal as Galactic in origin by searching for the expected anisotropy in the recoil directions. In statistical terms the question posed at this point is 'Is the distribution of observed recoil directions isotropic?', more specifically 'How many events are required to reject the hypothesis of isotropy (at a given confidence level)?'. Thirdly, assuming anisotropy is detected, the experiment would then collect more data and try and determine the form of the recoil anisotropy and hence the local WIMP velocity distribution. The halo models considered in Sec. II A lead us to consider two simple hypotheses to test: 1) Does the distribution of recoil directions show evidence of flattening (i.e. a non-spherical halo)? and 2) Does the distribution of recoil directions show evidence for a signal from the Sagittarius dwarf tidal stream?

As discussed in Sec. I, previous work aimed at determining the number of events required to detect the anisotropy in the recoil directions has indicated that 5 – 30 events are required to give a 90-95% rejection

<sup>3</sup> This package was not designed to model recoils in gaseous targets, however it accurately reproduces the recoil ranges in S found experimentally.

<sup>4</sup> Carbon recoils are ignored as they account for less than 1 % of the recoil rate due to the  $A^2$  dependence of the recoil rate and the low Carbon mass fraction.

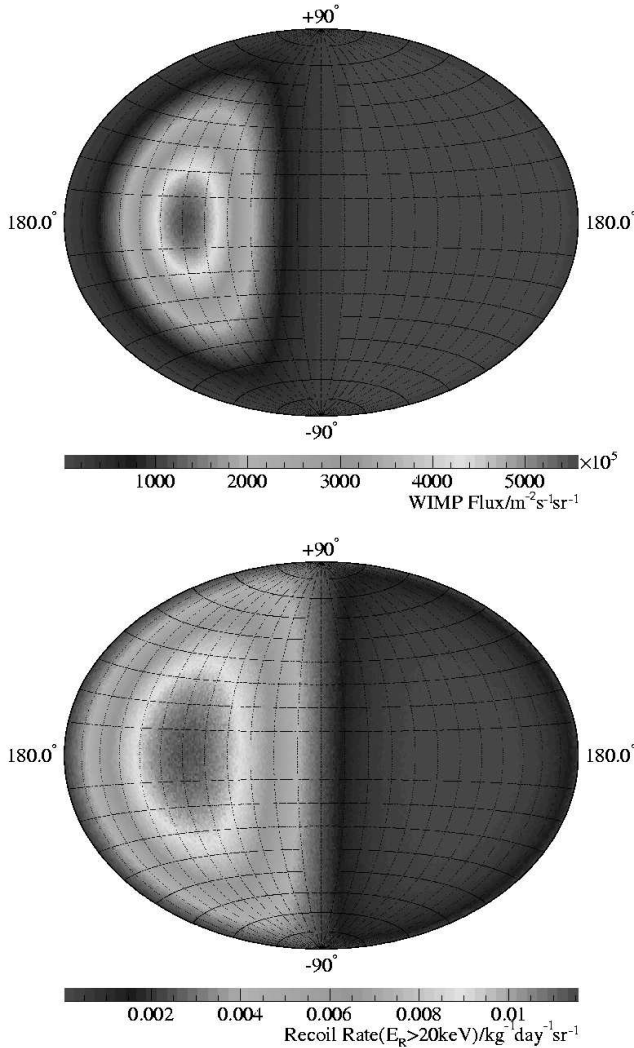


FIG. 1: Time averaged WIMP flux (top) and S Recoil rate above 20 keV (bottom) in Galactic  $(l, b)$  co-ordinates for halo model 1 and  $\rho_0 = 0.3 \text{ GeV cm}^{-3}$ ,  $m_\chi = 100 \text{ GeV}$  and  $\sigma_{\chi p} = 10^{-6} \text{ pb}$ .

of isotropy [19, 20]. However, these analyses suffer from several non-optimal features. Neither analysis took into account the angular resolution of the recoil reconstruction or the possibility that the absolute signs of the recoil vectors (i.e. their ‘sense’  $+\vec{x}$  or  $-\vec{x}$ ) may not be measurable. In Ref. [20], a Kolmogorov-Smirnov goodness of fit test was applied to the binned distribution of recoil  $\cos \gamma$  values, where  $\gamma$  is the angle between the recoil direction and the direction of motion of the Sun. Given the small number of events expected at the confirmation stage of an experiment, binning data can lead to a significant loss of information and should therefore be avoided. Ref. [19] used an unbinned likelihood analysis to determine the number of events required for a 95% confidence detection of isotropy in 95% of experiments, for a range of halo models, and also the number of events required to distinguish a triaxial halo from the standard maxwellian halo

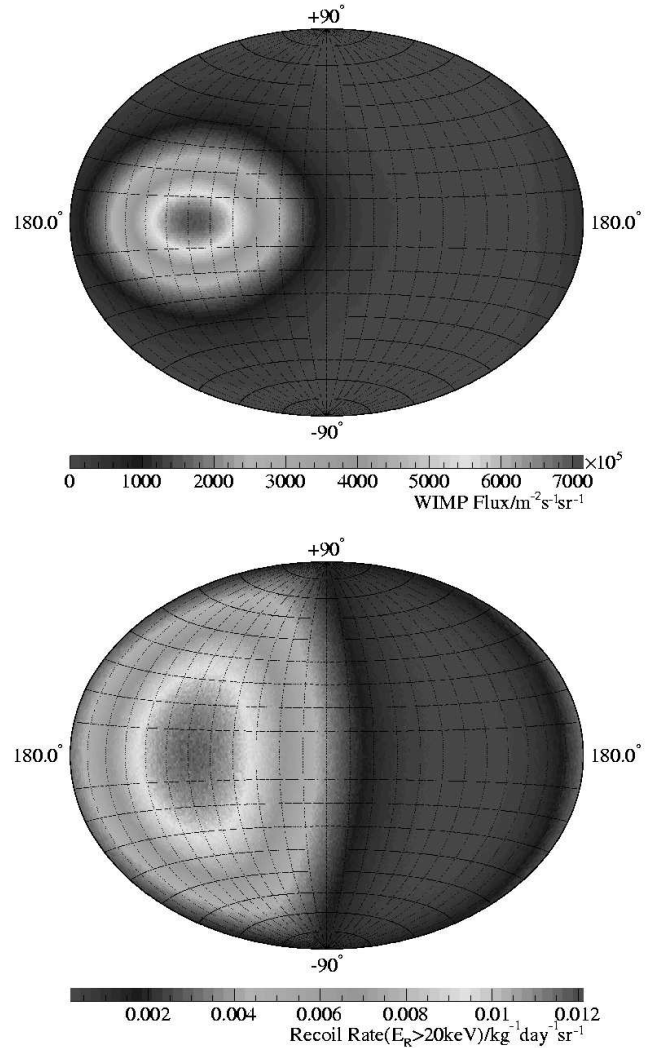


FIG. 2: As Fig. 1 for model 3 (logarithmic ellipsoidal model with  $p = 0.9$ ,  $q = 0.8$  and  $\beta = 0.4$ ).

model. The draw-back of likelihood analysis is that it only gives the relative likelihood of specific models (and parameter values), and there is no guarantee that any of the halo models considered is a good approximation to the local WIMP velocity distribution (especially since non-spherical and/or anisotropic halo models involve assumptions, which may or not be valid). As such this analysis could not be applied to real data.

Recoil directions constitute vectors, or, if the senses are unknown, undirected lines or axes, and so can equivalently be represented as points on a sphere. This allows us to use statistical inference methods developed for the analysis of spherically distributed data (for a review of this extensive field see the standard texts such as [46, 47]). We investigate a variety of non-parametric statistics designed to test the isotropy (Secs. III A and III B), rotational symmetry (Sec. III C) and median direction (Sec. III D). When quoting results for the num-

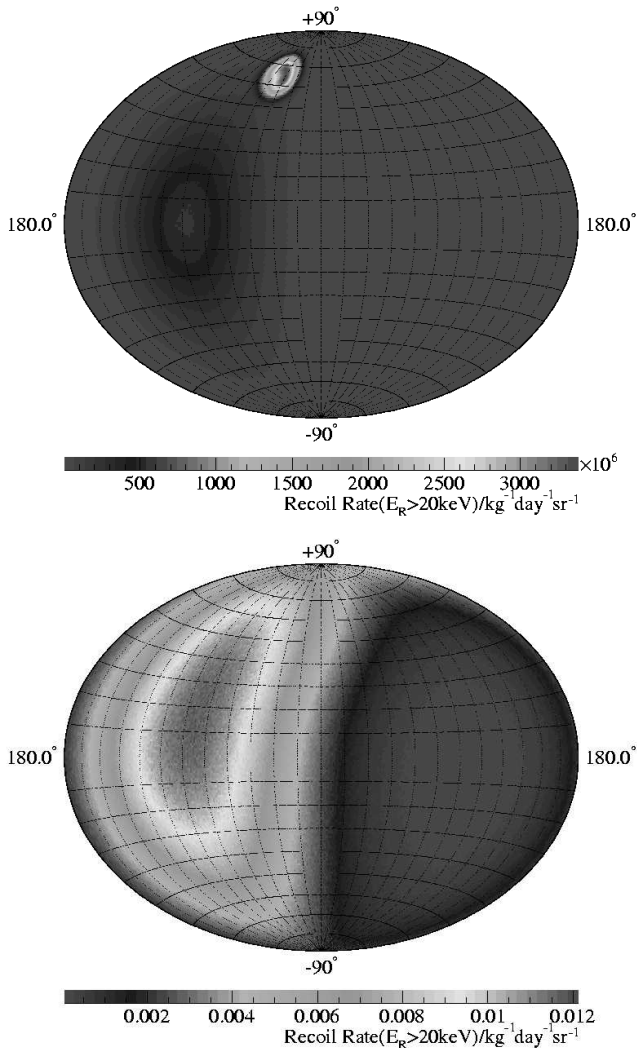


FIG. 3: As Fig. 1 for model 12 (standard halo model with a 25% contribution to the local WIMP density from the Sagittarius dwarf tidal stream).

bers of events required for detection, we focus on the benchmark halo models discussed in Sec. II A, however these tests do not make any assumptions about the form of the recoil spectrum and are hence equally applicable to any local WIMP velocity distribution.

### A. Coordinate system independent tests of isotropy

The first fundamental question posed by a directional detector observing an anomalous recoil signal is ‘Are the observed recoil directions consistent with an isotropic distribution?’. The most general tests of isotropy are those which do not depend on the coordinate system in which the sample vectors/axes are measured. This independence from the coordinate system means no assumption about the form of the anisotropy in the signal is required.

#### 1. Rayleigh-Watson statistic

The simplest coordinate independent statistic for vectorial data is the so-called modified Rayleigh-Watson statistic  $\mathcal{W}^*$ <sup>5</sup>. For a sample of  $N$  unit vectors  $\vec{x}_i$ ,  $\mathcal{W}^*$  is defined as [46, 48, 49]

$$\mathcal{W}^* = \left(1 - \frac{1}{2N}\right) \mathcal{W} + \frac{1}{10N} \mathcal{W}^2, \quad (5)$$

where  $\mathcal{W}$  is the (unmodified) Rayleigh-Watson statistic

$$\mathcal{W} = \frac{3}{N} \mathcal{R}^2, \quad (6)$$

and  $\mathcal{R}$  is the Rayleigh statistic:

$$\mathcal{R} = \left| \sum_{i=1}^N \vec{x}_i \right|. \quad (7)$$

The value of  $\mathcal{W}^*$  becomes larger as the degree of anisotropy increases and for isotropically distributed vectors,  $\mathcal{W}^*$  is asymptotically distributed as  $\chi_3^2$  [48, 49].

We find, using Monte Carlo simulations, that the difference between  $\chi_3^2$  and the true distribution of  $\mathcal{W}^*$  for isotropic vectors in the large  $\mathcal{W}^*$  tail of the distribution is less than 2% for  $N > 30$ . For  $N < 30$  the  $\chi_3^2$  distribution significantly underestimates the true probability distribution and we calculate the probability distribution from the exact probability distribution of  $\mathcal{R}$ , as described in Ref. [50].

#### 2. Bingham statistic

The Rayleigh-Watson statistic has the drawback that it is not sensitive to distributions which are symmetric with respect to the centre of the sphere. This property means that it cannot be used with axial data i.e. if the senses of the nuclear recoils are not known. An alternative statistic which avoids this problem is the Bingham statistic  $\mathcal{B}^*$  which is based on the scatter (or orientation) matrix  $\mathbf{T}$  of the data, defined as [46, 49, 51]

$$\mathbf{T} = \frac{1}{N} \sum_{i=1}^N \begin{pmatrix} x_i x_i & x_i y_i & x_i z_i \\ y_i x_i & y_i y_i & y_i z_i \\ z_i x_i & z_i y_i & z_i z_i \end{pmatrix}, \quad (8)$$

where  $(x_i, y_i, z_i)$  are the components of the  $i$ -th vector or axis. This matrix is real and symmetric with unit trace, so that that the sum of its eigenvalues  $e_k$  ( $k = 1, 2, 3$ ) is

<sup>5</sup> This modified statistic, and the others considered in this section, have the advantage of approaching their large  $N$  asymptotic distribution for smaller  $N$  than the unmodified statistic.

unity, and for an isotropic distribution all three eigenvalues should, modulo statistical fluctuations, be equal to 1/3. Bingham's modified statistic  $\mathcal{B}^*$  [46, 49, 52]

$$\mathcal{B}^* = \mathcal{B} \left( 1 - \frac{1}{N} \left[ \frac{47}{84} + \frac{13}{147} \mathcal{B} + \frac{5}{5292} \mathcal{B}^2 \right] \right), \quad (9)$$

where  $\mathcal{B}$  is the (unmodified) Bingham statistic

$$\mathcal{B} = \frac{15N}{2} \sum_{k=1}^3 \left( e_k - \frac{1}{3} \right)^2, \quad (10)$$

measures the deviation of the eigenvalues  $e_k$  from the value expected for an isotropic distribution. Note that  $\mathcal{B}^*$  can be calculated for axes (i.e. undirected lines  $\pm \vec{x}$ ) as well as vectors since  $\mathbf{T}$  is symmetric under a sign change of  $\vec{x}$ . For isotropically distributed vectors/axes  $\mathcal{B}^*$  is asymptotically distributed as  $\chi_5^2$ , and we have found, via Monte Carlo simulations, that the difference between the underlying probability distribution and  $\chi_5^2$  in the large  $\mathcal{B}^*$  tail of the distribution is always less than 10% and is less than 2% for  $N > 10$ .

### 3. Beran and Giné statistics

The most general test of the uniformity of a sample of  $N$  unit vectors or axes is provided by the statistics of Beran [53] and Giné [54], which are defined as

$$\mathcal{A} = N - \frac{4}{N\pi} \sum_{i=1}^{N-1} \sum_{j=i+1}^N \psi_{ij}, \quad (11)$$

$$\mathcal{G} = \frac{N}{2} - \frac{4}{N\pi} \sum_{i=1}^{N-1} \sum_{j=i+1}^N \sin \psi_{ij}, \quad (12)$$

where  $\psi_{ij}$  is the angle between the  $i$ -th and  $j$ -th directions. Beran's statistic  $\mathcal{A}$  tests for distributions which are asymmetric with respect to the centre of the sphere, and Giné's statistic  $\mathcal{G}$  tests for distributions which are symmetric with respect to the centre of the sphere. A suitable statistic for testing uniformity against all possible alternatives is therefore the combination  $\mathcal{F} = \mathcal{A} + \mathcal{G}$  [47]. In the case of axial data  $\mathcal{G}$  alone is a suitable test statistic.

The asymptotic distributions of  $\mathcal{A}$ ,  $\mathcal{G}$  and  $\mathcal{F}$  have not, to date, been calculated. We therefore generate the probability distributions for these statistics under the null hypothesis via Monte Carlo simulation.

## B. Coordinate system dependent tests

While coordinate frame independence is usually an advantage, the coordinate independent tests cannot make use of any information that is available about the expected form of the anisotropy. If the local WIMP distribution is smooth then the year averaged recoil flux is

peaked in the direction of the Sun's motion at  $(l_\odot, b_\odot) = (87.5^\circ, 1.3^\circ)$ . In this case, a suitable test statistic for vectorial data is [55]

$$\langle \cos \theta \rangle = \frac{\sum_{i=1}^N \cos \theta_i}{N}, \quad (13)$$

and for axial data

$$\langle |\cos \theta| \rangle = \frac{\sum_{i=1}^N |\cos \theta_i|}{N}, \quad (14)$$

where  $\theta_i$  is the angle between  $(l_\odot, b_\odot)$  and the  $i$ th vector/axis. For  $N$  isotropic vectors  $\langle \cos \theta \rangle$  ( $\langle |\cos \theta| \rangle$ ) can take values on the interval  $[-1, 1]$  ( $[0, 1]$ ) and, due to the central limit theorem, has a gaussian distribution with mean 0 (0.5) and variance  $1/3N$  ( $1/3N$ ) [55]. The larger the concentration of recoil directions towards  $(l_\odot, b_\odot)$  the larger these statistics will be. Conversely, if the anisotropy is oriented at an angle of  $90^\circ$  ( $45^\circ$ ) with respect to  $(l_\odot, b_\odot)$  then the resultant distribution of  $\langle \cos \theta \rangle$  ( $\langle |\cos \theta| \rangle$ ) will be indistinguishable from the isotropic case.

We calculate the probability distribution function of  $\langle \cos \theta \rangle$  and  $\langle |\cos \theta| \rangle$  as a function of  $N$  for the null hypothesis of an isotropic recoil spectrum using Monte Carlo simulations.

For each of the statistics discussed in Secs. III A and III B we determine the minimum number of events required to reject isotropy of recoil directions at 90 (95)% confidence in 90 (95)% of experiments (i.e. for rejection and acceptance probabilities of  $R_c = A_c = 0.9$  and 0.95),  $N_{\text{iso}}$ , as described in Appendix B for each statistic and halo model considered, including the detector response in the calculation of the recoil distributions. For the standard maxwellian halo model we also carry out the calculation neglecting the detector response, in order to assess its effect on the number of events required. The results are tabulated in Table II for each of the fiducial halo models for each statistic.

Overall, the two coordinate dependent tests of isotropy,  $\langle \cos \theta \rangle$  and  $\langle |\cos \theta| \rangle$ , have the lowest  $N_{\text{iso}}$  values and are thus the most powerful tests for rejecting isotropy. All the coordinate independent tests typically require 1.5-2 times more events to reject isotropy for a given halo model (for both vectorial and axial data). This behaviour is not surprising however, as the pole of the coordinate system chosen corresponds exactly to the peak anisotropy direction for the smooth halo models, however, the coordinate dependent tests are also the most powerful for rejecting isotropy in model 12 which includes a 25% contribution to the local WIMP density from the Sagittarius Dwarf tidal stream.

The vectorial coordinate independent tests ( $\mathcal{W}^*$ ,  $\mathcal{A}$  and  $\mathcal{F}$ ) all have very similar values of  $N_{\text{iso}}$  and are hence equally powerful for rejecting isotropy of recoils. The same is true of the axial coordinate independent tests ( $\mathcal{B}^*$  and  $\mathcal{G}$ ), however  $N_{\text{iso}}$  is of order ten times larger for

these tests than for the vectorial tests, and there is much greater variation between the fiducial halo models. Both of these effects are due to the form of the recoil direction distribution and the way in which lack of knowledge of the recoil sense changes this form. While most of the recoil arrival directions lie in the forward hemisphere,  $0 < l < 180^\circ$ , a non-negligible (halo model dependent) number lie in the backward hemisphere. For the vectorial tests, these backward events are not a problem as the tests can distinguish between the forward and backward hemispheres. When only the recoil axis is known, events in the backward hemisphere are effectively ‘added’ to the forward hemisphere, reducing the degree of anisotropy. Halo model 6 has the smallest rate in the backward hemi-

Halo Model	$N_{\text{iso}}$ for $(R_c, A_c) = (0.90, 0.90)$						
	Vectorial Statistics				Axial Statistics		
	$\mathcal{W}^*$	$\mathcal{A}$	$\mathcal{F}$	$\langle \cos \theta \rangle$	$\mathcal{B}^*$	$\mathcal{G}$	$\langle  \cos \theta  \rangle$
1	12	12	13	7	167	168	104
2	12	12	12	7	112	114	73
3	14	14	15	8	156	157	121
4	12	12	13	7	148	150	96
5	15	15	15	8	215	215	159
6	11	11	11	6	67	68	47
7	14	14	14	8	89	88	74
8	13	13	13	7	176	177	112
9	15	15	16	9	264	265	188
10	15	15	15	8	278	281	194
11	12	12	12	7	126	128	81
12	16	16	17	9	233	234	210

$N_{\text{iso}}$ for $(R_c, A_c) = (0.95, 0.95)$							
1	18	18	19	11	235	235	131
1 (no)	16	16	17	9	128	129	65
2	17	17	18	10	162	162	93
3	20	20	21	12	226	226	152
4	18	18	19	11	212	213	120
5	21	21	22	12	309	312	199
6	16	16	16	10	96	96	59
7	19	20	20	12	125	126	94
8	18	18	19	11	248	249	142
9	21	21	22	13	376	379	237
10	21	21	21	12	395	399	244
11	17	17	17	10	180	180	102
12	20	20	20	15	326	327	276

TABLE II: Number of recoil events required to reject isotropy of recoil directions,  $N_{\text{iso}}$ , at 90 (95)% confidence in 90 (95)% of experiments for each test statistic and halo model considered, including the uncertainty in the nuclear recoil reconstruction and for the standard halo model and  $A_c = R_c = 0.90$  ignoring the uncertainty in the nuclear recoil reconstruction (denoted by ‘no’ in the table). The test statistics have been divided into those suitable for vectorial data and those applicable to axial data (i.e. when the senses of the recoil directions are not known).

sphere and thus the lowest  $N_{\text{iso}}$  for both vectorial and axial tests, while model 10 has the largest backward rate and therefore has higher  $N_{\text{iso}}$  values with axial tests. In general the broader the local WIMP velocity distribution, the greater the number of events in the backward hemisphere, and hence a larger number of events are required to reject isotropy if the sense of the recoil directions are not known. We also see that while ignoring the detector response only marginally reduces the number of events required for the vectorial tests, the number of events required for the axial tests are increased by a factor of roughly two.

We now translate the number of events required to reject isotropy into the equivalent detector exposure,  $E$ , required to observe this number of events. If the sense of the recoil direction is observed, isotropy could be rejected at 95% confidence in 95% of experiments for  $\sigma_0 \sim 3 \times 10^{-9}$  pb and  $\rho_0 \sim 0.3 \text{ GeV cm}^{-3}$  with an exposure of  $E = 10^5 \text{ kg day}$ . For a detector only capable of measuring the recoil axes a  $10^5 \text{ kg day}$  exposure would be able to reject isotropy at the same confidence level and acceptance down to  $\sigma_0 \sim 3 \times 10^{-8}$  pb.

### C. Tests for rotational symmetry

Once an observed anomalous recoil signal is found to be incompatible (at some confidence level) with isotropy the next question to pose is ‘Is the observed distribution consistent with a spherical halo?’. A generic feature of triaxial halo models is a flattening of the recoil distribution towards the galactic plane, or more generally, flattened along one principal axis of the local velocity distribution. This type of distribution can be probed using tests for rotational symmetry about a specified direction or axis. In the case of smooth halo models this direction/axis is the direction of motion of the Earth through the MW halo. Over the year, this averages to the direction of motion of the Sun,  $(l_\odot, b_\odot) = (87.5^\circ, 1.3^\circ)$ <sup>6</sup>.

A test of rotational symmetry about some hypothesised direction  $(\theta_0, \phi_0)$  (valid for vectors or axes) can be performed by first rotating the sample vectors or axes so that their polar angles are measured relative to  $(\theta_0, \phi_0)$ . The resultant data are then sorted in ascending order of the normalised azimuthal angle so that

$$X_1 = \frac{\phi_1}{2\pi}, \dots, X_N = \frac{\phi_N}{2\pi}, \quad (15)$$

with  $X_1 < X_2 < \dots < X_N$ . For rotational symmetry, the distribution of  $X$  should be uniform between 0 and 1 so that the cumulative PDF,  $P(X) = X$ . This hypothesis can be tested by using the Kuiper statistic [47]. This test

<sup>6</sup> For experiments with an exposure that is non-uniform in time, the mean direction could be calculated by averaging the Earth’s velocity vector over the, time-dependent, exposure.



is related to the well-known Kolmogorov-Smirnov test, but has the advantage of being invariant under cyclic transformations and equally sensitive to deviations at all values of  $X$ . The modified Kuiper statistic is defined as

$$\mathcal{V}^* = \mathcal{V} \left( N^{1/2} + 0.155 + \frac{0.24}{N^{1/2}} \right), \quad (16)$$

where  $\mathcal{V}$  is the (unmodified) Kuiper statistic

$$\mathcal{V} = \mathcal{D}^+ + \mathcal{D}^-, \quad (17)$$

and

$$\mathcal{D}^+ = \max \left( \frac{i}{N} - F(X_i) \right), \quad i = 1, \dots, N \quad (18)$$

$$\mathcal{D}^- = \max \left( F(X_i) - \frac{i-1}{N} \right). \quad (19)$$

As there is no general formula for the distribution of  $\mathcal{V}^*$  under the null hypothesis of rotational symmetry, we use Monte Carlos to generate the null probability distribution assuming the standard halo model<sup>7</sup>. We focus here on the two fiducial halo models for which the recoil distribution deviates most from that produced by the standard halo model: the logarithmic ellipsoidal models 5 ( $p = 0.9$ ,  $q = 0.8$ ,  $\beta = 0.4$ , long axis) and 7 ( $p = 0.72$ ,  $q = 0.7$ ,  $\beta = 0.4$ , intermediate axis) (more spherical models that produce less flattened recoil distributions would have larger  $N_{\text{rot}}$ ). We find that halo model 5 has  $A < 0.4$  over a large range of  $N$  values, and of order 5000-8000 events would be required to reject rotational symmetry at 90 + % confidence with similar acceptance. In contrast for halo model 7 (which is more extreme)  $N_{\text{rot}} = 1170$  (1710) for  $R_c = A_c = 0.9$  (0.95). So while rotational symmetry of the recoil distribution can be rejected at high confidence and acceptance for this, rather extreme, halo model, it requires 10-50 times the number of events required to reject isotropy (depending on whether vectors or axes are measured in the latter case).

Converting these numbers to the equivalent exposures in kg day gives  $E(R_c = A_c = 0.9 \text{ (0.95)}) = 7.8 \text{ (11)} \times 10^{-3} \sigma_0^{-1} \rho_0^{-1}$ . Hence for the  $10^5$  kg day exposure considered in the previous subsection, rotational symmetry could be rejected at 90% confidence down to  $\sigma_0 \sim 3 \times 10^{-7}$  pb for  $\rho_0 \sim 0.3 \text{ GeV cm}^{-3}$ , independent of whether the senses of the recoils can be measured. The sensitivity of a TPC-based directional detector for rejecting a spherical halo if the real MW halo is significantly triaxial using this statistic, is therefore several orders of magnitude lower than for rejecting isotropy of recoil directions. Devising other tests that may be a more powerful probe of the flattening of the recoil distribution produced by non-spherical halo models is therefore an important task.

<sup>7</sup> This may appear to introduce a model dependence into the test, however any other distribution rotationally symmetric about  $(l_\odot, b_\odot)$  would give the same null distribution for  $\mathcal{V}^*$ .

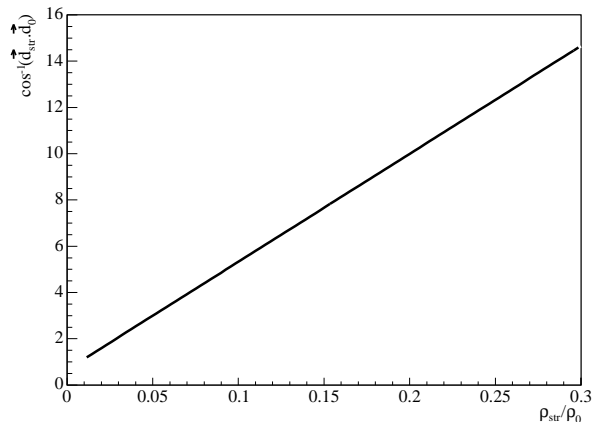


FIG. 4: Variation of the angle between the mean recoil directions of the standard halo and the standard halo plus the Sagittarius tidal stream as a function of the fraction of the local WIMP density contributed by the stream,  $\rho_{\text{str}}/\rho_0$ .

#### D. Tests for mean direction

The Sagittarius dwarf tidal stream is expected to have a velocity dispersion which is small compared to its velocity relative to the solar system [39, 40] and therefore the recoil distribution due to WIMPs from the stream will be peaked in the hemisphere whose pole points in the direction of the stream velocity. The net (stream plus smooth background WIMP distribution) peak direction depends on the fraction of the local density that the tidal stream contributes. Fig. 4 shows the angle between the direction of the Sun's motion  $(l_\odot, b_\odot) = (87.5^\circ, 1.3^\circ)$  and the direction of the peak in the recoil distribution produced by a maxwellian halo plus the Sagittarius stream as a function of the local WIMP density contributed by the stream. For the  $\rho_{\text{str}}/\rho_0 \sim 1 - 30\%$  range of stream densities suggested by [39, 40], the angle is in the range  $2 - 15^\circ$ . This feature suggests that the presence of the Sagittarius tidal stream in the solar neighbourhood could be tested for by comparing the median direction of the observed recoil vectors with the (known) direction of solar motion.

For vectorial data, the median direction is defined as that direction  $(\hat{\theta}, \hat{\phi})$  which minimises the sum of ar-lengths between  $(\hat{\theta}, \hat{\phi})$  and the sample vectors [47], and can found by minimising the quantity

$$\mathcal{M} = \sum_{i=1}^N \cos^{-1}(\hat{x}x_i + \hat{y}y_i + \hat{z}z_i), \quad (20)$$

while for axial data an estimate of the principal axis of the distribution is provided by the eigenvector corresponding to the largest eigenvalue of the scatter matrix  $\mathbf{T}$ . A test of compatibility between the measured median direction and a hypothesised median direction  $(\theta_0, \phi_0)$  for vectorial data can be performed [47] by first rotating the

data so that the polar angles are measured relative to a pole in the direction of the sample median  $(\hat{\theta}, \hat{\phi})$  using the matrix

$$\mathbf{A}(\theta, \phi) = \begin{pmatrix} \cos \hat{\theta} \cos \hat{\phi} & \cos \hat{\theta} \sin \hat{\phi} & -\sin \hat{\theta} \\ -\sin \hat{\phi} & \cos \hat{\phi} & 0 \\ \sin \hat{\theta} \cos \hat{\phi} & \sin \hat{\theta} \sin \hat{\phi} & \cos \hat{\theta} \end{pmatrix}. \quad (21)$$

The matrix  $\Sigma$

$$\Sigma = \frac{1}{2} \begin{pmatrix} \sigma_{11} & \sigma_{12} \\ \sigma_{21} & \sigma_{22} \end{pmatrix}, \quad (22)$$

where

$$\sigma_{11} = 1 + \frac{1}{N} \sum_{i=1}^N \cos 2\phi'_i, \quad (23)$$

$$\sigma_{22} = 1 - \frac{1}{N} \sum_{i=1}^N \cos 2\phi'_i, \quad (24)$$

$$\sigma_{12} = \sigma_{21} = \frac{1}{N} \sum_{i=1}^N \sin 2\phi'_i, \quad (25)$$

is then calculated from the rotated sample vectors and the sample vectors are rotated again so that their polar angles are measured relative to a pole in the direction of the hypothesised median using the matrix  $\mathbf{A}(\theta_0, \phi_0)$  and the vector

$$\vec{U} = N^{-1/2} \begin{pmatrix} \sum \cos \phi_i^0 \\ \sum \sin \phi_i^0 \end{pmatrix}, \quad (26)$$

where  $\phi_i^0$  is the azimuthal angle of the  $i$ th sample vector relative to a pole at  $(\theta_0, \phi_0)$  is calculated. Finally the statistic  $\mathcal{X}^2$ , defined as

$$\mathcal{X}^2 = \vec{U}^T \Sigma^{-1} \vec{U}, \quad (27)$$

is calculated. This statistic is distributed as  $\chi^2_2$  for samples drawn from a distribution with median direction  $(\theta_0, \phi_0)$ .

For  $\rho_{\text{str}}/\rho_0 = 25\%$  (which is at the upper end of the range of values suggested in [39, 40], and therefore provides a lower limit on the number of events required), we find that the minimum number of events required to reject  $(l_\odot, b_\odot)$  as the median direction,  $N_{\text{dir}}$ , is 201 (294) for  $R_c = A_c = 0.9$  (0.95). Comparing these numbers with those required to reject isotropy of recoils for this stream density, it can be seen that  $\sim 10 - 20$  times more events are needed to reject the direction of the solar motion as the median recoil direction. In terms of exposure, these numbers of events would be achievable with a  $10^5$  kg day exposure for WIMP-proton cross sections down to  $\sigma_0 \sim 4 \times 10^{-8}$  ( $6 \times 10^{-8}$ ) pb for  $\rho_0 = 0.3 \text{ GeV cm}^{-3}$ .

In the case of axial recoil directions, the  $\mathcal{X}^2$  test cannot be applied, however, the rotational symmetry test of Sec. III C can be used since the recoil distribution will not

be rotationally symmetric about  $(l_\odot, b_\odot)$  in the presence of the Sagittarius stream. Using the statistic  $\mathcal{V}^*$  we find  $N_{\text{rot}} = 390$  (574) for  $R_c = A_c = 0.9$  (0.95). These numbers are roughly twice those for the  $\mathcal{X}^2$  test, and also for rejecting isotropy with axial data. Thus with only axial data, a  $10^5$  kg day exposure would be sufficient to identify the presence of the Sagittarius tidal stream comprising 25% of the local WIMP density for WIMP-proton cross sections down to  $\sigma_0 \sim 8 \times 10^{-8}$  ( $1 \times 10^{-7}$ ) pb and  $\rho_0 = 0.3 \text{ GeV cm}^{-3}$ .

We caution that these numbers have been calculated for parameter values at the optimistic ends of the ranges estimated in Ref. [39, 40], i.e. high density and low velocity dispersion. A lower stream density and/or a higher velocity dispersion would give a peak recoil direction closer to the mean direction of motion of the Sun, and make the deviation due to the stream harder to detect. For the most pessimistic case of  $\rho_{\text{str}}/\rho_0 = 0.003$  and  $\sigma_{\text{str}} = 70 \text{ kms}^{-1}$ , the net WIMP flux and recoil rate are virtually indistinguishable from those for the standard halo model and tens of thousands of events would be needed to detect the stream. In general the detectability of cold streams of WIMPs will clearly depend on how much their bulk velocity deviates from the direction of solar motion.

#### IV. DISCUSSION

We have studied the application of non-parametric tests, developed for the analysis of spherical data [46, 47], to the analysis of simulated data as expected from a TPC-based directional WIMP detector [17, 18], taking into account the uncertainties in the reconstruction of the nuclear recoil directions. These tests, unlike likelihood analysis, do not require any assumptions about the form of the local WIMP velocity distribution. This is advantageous as even if the properties (i.e. shape, velocity anisotropy, and density profile) of the MW halo at the solar radius were accurately determined there would likely be a wide range of local velocity distributions consistent with these properties.

For a range of fiducial anisotropic and/or triaxial halo models, with parameters chosen to reproduce the range of properties found in simulations/observations of dark matter halos, we calculate the number of events required to distinguish the WIMP directional signal from an isotropic background using a variety of tests. The most powerful test is the, co-ordinate system dependent, test of the mean angle between the observed nuclear recoils and the direction of motion of the Sun, which takes advantage of the fact that, for a smooth halo, the recoil rate is peaked in the direction of the Sun's motion. We find that if the senses of the recoils are known then of order ten events will be sufficient to distinguish a WIMP signal from an isotropic background for all of the halo models considered, with the uncertainties in reconstructing the recoil direction only mildly increasing the

required number of events. If the senses of the recoils are not known the number of events required is an order of magnitude larger, with a large variation between halo models and the recoil resolution is now an important factor. The number of events required would be significantly larger if the WIMP velocity distribution *in the rest frame of the detector* is close to isotropic [19], which could be the case if the MW halo is co-rotating or if the local dark matter density has a significant contribution from a cold flow with direction so as to cancel out the front-rear asymmetry from the smooth background distribution [56], however for halos formed hierarchically (as is the case in Cold Dark Matter cosmologies) neither of these possibilities are expected to occur (see e.g. Ref. [23, 35]). We find that distinguishing between halo models, in particular determining whether the MW halo is (close to) spherical, using tests of rotational symmetry will require thousands of events. This is in broad agreement with the results of Ref. [19].

Gondolo has shown that the recoil momentum spectrum is the Radon transform of the WIMP velocity distribution [57]. In theory the transform could be inverted to directly measure the WIMP velocity distribution from the measured recoil momentum distribution, however the inversion algorithms available in the literature require large numbers of events [57]. Furthermore, as we have shown, the uncertainties in the reconstruction of the recoil directions due to multiple scattering and diffusion have a significant effect on the observed recoil distribution. Developing techniques to distinguish between the recoil distributions expected from different halo models, for finite amounts of data and taking into account the experimental resolution, is therefore of key importance for the full astronomical exploitation of data from directional detectors.

If a significant fraction of the local dark matter is in a cold flow (with velocity dispersion far smaller than its bulk velocity) then the peak recoil direction will deviate from the direction of the solar motion. In fact the Sagittarius tidal stream is thought to pass through the solar neighbourhood [37, 38], and using values for the properties of the stream at the optimistic end of the ranges estimated in Ref. [39, 40] this deviation could be detected with of order a hundred events even if the sense of the nuclear recoils is not measurable. This illustrates that if the Galactic dark matter is in the form of WIMPs then WIMP directional detectors, such as DRIFT [17, 18], will be able to do ‘WIMP astronomy’.

### Acknowledgments

A.M.G was supported by PPARC and the Swedish Research Council. B.M. was supported by PPARC.

We are grateful to John McMillan, Nick Cox and Toby Lewis for useful discussions.

### APPENDIX A: ORBITAL VELOCITY OF THE EARTH

The Earth’s orbit around the Sun lies in the Ecliptic plane and is approximately circular with eccentricity  $e = 0.0167$  and semi-major axis  $a = 1.000 \text{ AU} = 1.496 \times 10^{11} \text{ m}$ . The tangential and radial components of the Earth’s orbital velocity at a given time  $t$  are calculated from [58]

$$\begin{aligned} v_T(t) &= \frac{2\pi a(1 + e \cos \nu(t))}{P\sqrt{1 - e^2}}, \\ v_R(t) &= \frac{2\pi a e \sin \nu(t)}{P\sqrt{1 - e^2}}, \\ \nu(t) &= \lambda_\odot(t) - \varpi - \pi, \end{aligned} \quad (\text{A1})$$

where  $\lambda_\odot(t)$  is the ecliptic longitude of the Sun,  $\varpi = 103^\circ$  [59] is the argument of perihelion of the Earth and  $P$  is the orbital period. The Solar ecliptic longitude at time  $t$ , accurate to  $0.01^\circ$  for  $t$  between 1950 and 2050, is calculated from [59]  $\lambda_\odot(t) = 280.460 + 0.9856474t + 1.915 \sin g + 0.020 \sin 2g$  where  $t$  is the time given in terms of the Julian Day  $JD$  via  $t = JD - 2451545.0$  and  $g$  is the mean anomaly of the orbit given by  $g = 357.528 + 0.9856003t$ . Using Eqs. A1, the Earth’s orbital velocity in the Ecliptic coordinate system is calculated as

$$\vec{v}_{\text{orb}}^E(t) = \begin{pmatrix} \mathcal{A}(t)v_R(t) - \mathcal{B}(t)v_T(t) \\ \mathcal{A}(t)v_T(t) - \mathcal{B}(t)v_R(t) \\ 0 \end{pmatrix}, \quad (\text{A2})$$

$$(\text{A3})$$

where

$$\mathcal{A}(t) = \cos \nu(t) \cos \varpi - \sin \nu(t) \sin \varpi, \quad (\text{A4})$$

$$\mathcal{B}(t) = \sin \nu(t) \cos \varpi - \cos \nu(t) \sin \varpi. \quad (\text{A5})$$

This velocity is then transformed to the galactic coordinate system via the rotations

$$\vec{v}_{\text{orb}}(t) = \mathbf{G} \mathbf{E} \vec{v}_{\text{orb}}^E(t), \quad (\text{A6})$$

with rotation matrices

$$\mathbf{E} = \begin{pmatrix} 1 & 0 & 0 \\ 0 & \cos \epsilon & \sin \epsilon \\ 0 & -\sin \epsilon & \cos \epsilon \end{pmatrix}, \quad (\text{A7})$$

where  $\epsilon = 23.5^\circ$  is the obliquity of the ecliptic plane to the equatorial plane of the Earth [59] and [58]

$$\mathbf{G} = \begin{pmatrix} -0.054876 & -0.873437 & -0.483835 \\ 0.494109 & -0.444830 & 0.746982 \\ -0.867666 & -0.198076 & 0.455984 \end{pmatrix}. \quad (\text{A8})$$

## APPENDIX B: HYPOTHESIS TESTING

For each halo model considered we use Monte Carlo simulations to generate  $N$  recoil scattering events in each of  $10^5$  experiments, for values of  $N$  between 5 and 400 (the lower value corresponding to the point at which an anomalous recoil signal would first be identified at high confidence). The background in each experiment is assumed to be zero, which is a reasonable expectation for experiments such as DRIFT-II [60]. For each experiment the test statistic  $\mathcal{T}$  is calculated from the  $N$  recoil directions used to give the probability distribution of the statistic,  $p_1(\mathcal{T}; N)$ , as a function of the number of recoil events. The probability distribution for the null hypothesis of isotropy,  $p_0(\mathcal{T}; N)$ , is calculated using analytical expression where available and otherwise via Monte Carlo simulations. As in standard hypothesis testing, the overlap between these two distributions allows the probability<sup>8</sup> with which the null and alternative hypotheses can be rejected or accepted to be calculated. For a given value  $\mathcal{T}_g$ , the rejection factor  $R$  is the probability of measuring  $\mathcal{T} \leq \mathcal{T}_g$  if the null hypothesis is true:

$$R = \int_0^{\mathcal{T}_g} p_0(\mathcal{T}; N) d\mathcal{T}. \quad (\text{B1})$$

The rejection factor thus gives the confidence level with which the null hypothesis can be rejected given a particular value of the test statistic  $\mathcal{T} = \mathcal{T}_g$ . For the same value of the test statistic  $\mathcal{T}_g$ , the acceptance factor  $A$  is<sup>8</sup> We use the frequentist definition of ‘probability’ throughout.

the probability of measuring  $\mathcal{T} \geq \mathcal{T}_g$  if the alternative hypothesis is true

$$A = \int_{\mathcal{T}_g}^{\infty} p_1(\mathcal{T}; N) d\mathcal{T}. \quad (\text{B2})$$

Equivalently, under the frequentist definition of probability, it is the fraction of experiments in which the alternative hypothesis is true that measure  $\mathcal{T} \geq \mathcal{T}_g$  and thus reject the null hypothesis at confidence level  $R$ .

By calculating  $R$  and  $A$  from the probability distributions of the test statistic for the null and alternative hypothesis as a function of  $N$ , an ‘acceptance-rejection’ plot can be built up for each value of  $N$  and for any given level of rejection,  $R_c$ , the level of acceptance  $A_c$  achievable for each recoil sample size  $N$  calculated. In other words we find the  $N$  such that ‘for  $N$  observed recoils, the null hypothesis is rejected at the  $100R_c\%$  confidence level in  $100A_c\%$  of experiments in which the alternative hypothesis is true’.

Clearly, a high value of  $R_c$  is required to reject the null hypothesis at high confidence. A high acceptance is also required; if, for instance,  $A_c = 0.1$  then only 1 in 10 experiments will be able to reject the null hypothesis at the given  $R_c$ , furthermore if  $A_c$  is low, the null hypothesis could sometimes be erroneously rejected at a given confidence level with a low number of events due to statistical fluctuations. We therefore use  $A_c = R_c = 0.9$  (0.95) as our criteria, and calculate the corresponding minimum number of events required.

- 
- [1] A. K. Drukier, K. Freese and D. N. Spergel, Phys. Rev. D **33**, 3495 (1986); K. Freese, J. Frieman and A. Gould, Phys. Rev. D **37**, 3388 (1988).
  - [2] D. N. Spergel, Phys. Rev. D **37**, 1353 (1988).
  - [3] G. Jungman, M. Kamionkowski and K. Griest, Phys. Rep. **267**, 195 (1996).
  - [4] J. D. Lewin and P. F. Smith, Astropart. Phys. **6**, 87 (1996).
  - [5] R. Bernabei et al., Phys. Lett. **B389**, 757 (1996); ibid **B408**, 439 (1997); ibid **B424**, 195 (1998); ibid **B450**, 448 (1999); ibid **B480**, 23 (2000); Riv. Nuovo. Cim. **26N1** 1 (2003), astro-ph/0307403.
  - [6] D. Akerib et al., astro-ph/0405033; A. Benoit et al., Phys. Lett. **B545**, 43 (2002); N. J. Smith et al., proceedings of 4th Int. Workshop on Identification of Dark Matter (York, 2002) ed. N. J. C. Spooner and V. Kudryavtsev, World Scientific, Singapore (2003).
  - [7] M. Brhlik and L. Roszkowski, Phys. Lett. **B464**, 303 (1999), astro-ph/9903468; G. Gelmini and P. Gondolo, hep-ph/0405278.
  - [8] P. Belli et al., Phys. Rev. D **61**, 023512 (2000), hep-ph/0203242; C. J. Copi and L. M. Krauss, Phys. Rev. D **67**, 103507, (2003) astro-ph/0208010, N. Fornengo and S. Scopel, Phys. Lett. B **576**, 189 (2003), hep-ph/0301132.
  - [9] A. M. Green, Phys. Rev. D **63**, 043005 (2001), astro-ph/0008318.
  - [10] A. M. Green, Phys. Rev. D **68**, 023004 (2003), astro-ph/0304446.
  - [11] P. Ullio, M. Kamionkowski and P. Vogel, JHEP **0107**, 044 (2001), hep-ph/0010036, A. Kurylov and M. Kamionkowski, Phys. Rev. D **69**, 063503 (2004), hep-ph/0307185.
  - [12] D. Smith and N. Weiner, Phys. Rev. D **64**, 043502 (2001), hep-ph/0101138; D. Smith and N. Weiner, hep-ph/0402065.
  - [13] B. Morgan et al., Proceedings of The International Workshop on Technique and Application of Xenon Detectors, Tokyo, Japan 2000, p78 eds. Y. Suzuki, M. Nakahata, Y. Koshio and S. Moriyama, World Scientific (2002); B. Morgan, Nucl. Inst. and Meth. A **513**, 226 (2003).
  - [14] S. R. Bandler et al., Phys. Rev. Lett. **74**, 3169 (1995).
  - [15] R. J. Gaitskell et al., Nucl. Inst. and Meth. A **370**, (1996).
  - [16] H. Sekiya et al., Phys. Lett. B **571**, 132 (2003); H. Sekiya et al., to appear in proceedings of 5th workshop on Neutrino Oscillations and their Origin (NOON2004), astro-ph/0405598.
  - [17] D. P. Snowden-Ifft, C. J. Martoff, and J. M. Burwell, Phys. Rev. D **61**, 1 (2000), astro-ph/9904064.
  - [18] G. J. Alner et al., to appear in Nucl. Inst. and Meth. A.

- [19] C. J. Copi, J. Heo and L. M. Krauss, Phys. Lett. B **461**, 43 (1999), [astro-ph/9904499](#); C. J. Copi and L. M. Krauss, Phys. Rev. D **63**, 043507 (2001), [astro-ph/0009467](#).
- [20] M. J. Lehner et al., *Dark Matter in Astro and Particle Physics*, Proceedings of the International Conference DARK2000, Heidelberg, Germany, 2000, p590 ed. H. V. Klapdor-Kleingrothaus, Springer-Verlag (2001).
- [21] C. S. Frenk, S. D. M. White, M. Davis and G. Efstathiou, Astrophys. J. **237**, 507 (1988).
- [22] Y. P. Jing and Y. Suto, Astrophys. J. **574**, 538 (2002), [astro-ph/0202064](#).
- [23] B. Moore et al., Phys. Rev. D **64**, 063508 (2001), [astro-ph/0106271](#).
- [24] J. Dubinski and R. G. Carlberg, Astrophys. J. **378**, 496 (1991); S. Kazantzidis et al., [astro-ph/0405189](#).
- [25] P. D. Sackett, Galaxy Dynamics, ASP Conf Series, 182, p393, eds. D. Merritt, J.A. Sellwood and M. Valluri, (1999), [astro-ph/9903420](#); M. R. Merrifield, to appear in proceedings of IAU Symposium 220 'Dark Matter in Galaxies', Sydney, 2003 eds. D. J. Pisano, M. Walker and K. Freeman, Astron. Soc. Pacific (2004) [astro-ph/0310497](#).
- [26] J. J. Binney, Mon. Not. Roy. Astron. Soc. **196**, 455 (1981); P. T. de Zeeuw, and D. Pfenniger, Mon. Not. Roy. Astron. Soc. **235**, 949 (1988) Erratum: **262**, 1088.
- [27] N. W. Evans, C. M. Carollo and P. T. de Zeeuw, Mon. Not. Roy. Astron. Soc. **318**, 1131, (2000), [astro-ph/0008156](#).
- [28] L. P. Osipkov, Pis'ma Astron. Zh. **55**, 77 (1979).
- [29] D. Merritt, Astron. J. **90**, 1027 (1985).
- [30] P. Ullio and M. Kamionkowski, JHEP **0103**, 049 (2001), [hep-ph/0006183](#).
- [31] A. M. Green, Phys. Rev. D **66**, 083003 (2002), [astro-ph/0207336](#).
- [32] J. F. Navarro, C. S. Frenk and S. D. M. White, Astrophys. J. **462**, 563 (1996).
- [33] L. M. Widrow, Astrophys. J. Suppl. S. **131**, 39 (2000), [astro-ph/0003302](#).
- [34] D. Stiff, L. M. Widrow and J. Frieman, Phys. Rev. D **64**, 083516 (2001), [astro-ph/0106048](#).
- [35] A. Helmi, S. D. M. White and V. Springel, Phys. Rev. D **66**, 063502 (2002), [astro-ph/0201289](#).
- [36] D. Stiff and L. M. Widrow, Phys. Rev. Lett. **90**, 211301 (2003), [astro-ph/0301301](#).
- [37] S. R. Majewski et al., Astrophys. J. **599**, 1082 (2003), [astro-ph/0304198](#).
- [38] H. J. Newberg et al., Astrophys. J. **596**, L191 (2003), [astro-ph/0309162](#).
- [39] K. Freese, P. Gondolo and H. J. Newberg, [astro-ph/0309279](#).
- [40] K. Freese, P. Gondolo, H. J. Newberg and M. Lewis, Phys. Rev. Lett. **92**, 111301 (2004), [astro-ph/0310334](#).
- [41] R. Bellazzini and G. Spandre, Nucl. Inst. and Meth. A. **513**, 231, (2003).
- [42] T. Ohnuki, D. P. Snowden-Ifft and C. J. Martoff, Nucl. Inst. and Meth. A. **463**, 142, (2001).
- [43] J. F. Ziegler, J. P. Biersack and U. Littmark, *The stopping and range of ions in solids*, Pergamon Press (1985), <http://www.srim.org>.
- [44] J. Binney and S. Tremaine, *Galactic Dynamics*, Princeton University Press (1987).
- [45] W. Dehnen and J. J. Binney, Mon. Not. Roy. Astron. Soc. **298**, 387 (1998), [astro-ph/9710077](#).
- [46] K. V. Mardia and P. Jupp, *Directional Statistics*, Wiley, Chichester (2002).
- [47] N. I. Fisher, T. Lewis and B. J. J. Embleton, *Statistical analysis of spherical data*, CUP, (1987).
- [48] G. S. Watson, Geophys. Suppl. Mon. Not. Roy. Astron. Soc. **7**, 160 (1956).
- [49] G. S. Watson, *Statistics on Spheres*, Wiley, New York (1983).
- [50] M. A. Stephens, J. Amer. Statist. Assoc. **59**, 160 (1964).
- [51] G. S. Watson, J. Geol. **74**, 786 (1966).
- [52] C. Bingham, Ann. Stat. **2**, 1201 (1974).
- [53] R. Beran, J. App. Prob. **5**, 177 (1968).
- [54] E. M. Giné, Ann. Stat. **3**, 1243 (1975).
- [55] M. S. Briggs, Astrophys. J. **407**, 125, (1993).
- [56] P. Sikivie, I. I. Tkachev and Y. Wang, Phys. Rev. Lett. **75**, 2911 (1995), Phys. Rev. D **56**, 1863 (1997); P. Sikivie, Phys. Lett. B **432**, 139 (1998).
- [57] P. Gondolo, Phys. Rev. D **66**, 103513 (2002), [hep-ph/0209110](#).
- [58] R. M. Green, *Spherical Astronomy*, CUP (1993).
- [59] *The Astronomical Almanac for the year 2003*, United States Government Printing Office (2003).
- [60] J. Davies, private communication